## Supporting Information

# Pt Single Atoms Anchored on $CoO_X$ Nanoislands for Efficient Biomass-Derived 5-Methylfurfural Production

Xiongxin Liang[a], Zidong Huang[a], Xin Luo[a], Xu Yang[a,c,*], Dai Dang[a], Xu Li[b,*], Hongliang Peng[d]

[a] School of Chemical Engineering and Light Industry, Guangdong University of Technology, Guangzhou, 510006, P. R. China

[b] Laboratory of Electrochemical Energy Storage and Energy Conversion of Hainan Province, School of Chemistry and Chemical Engineering, Hainan Normal University, Haikou 571158, P. R. China

[c] Jieyang Branch of Chemistry and Chemical Engineering Guangdong Laboratory, Jieyang 515200, China

[d] Guangxi Key Laboratory of Information Materials, Guilin University of Electronic Technology, Guilin 541004, P.R. China

[*] Corresponding authors. E-mail: yangxu@gdut.edu.cn, 597764003@qq.com

## Figures and Tables

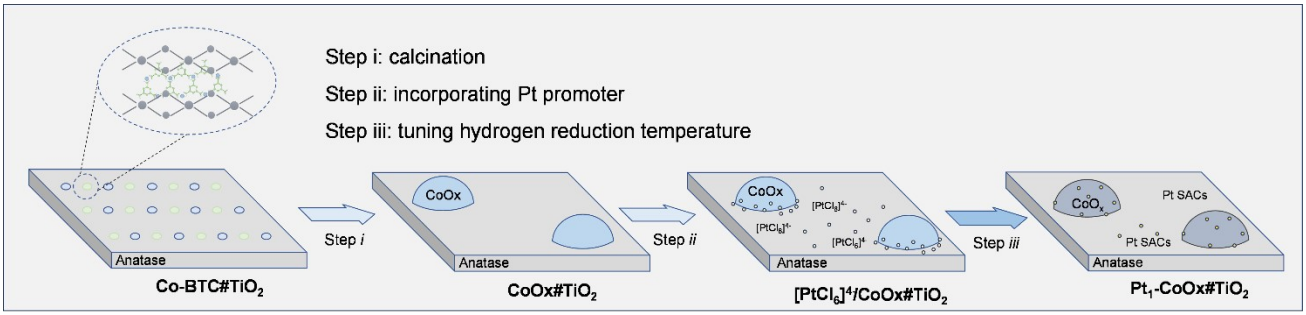


Scheme S1 Schematic illustration of the synthesis process.

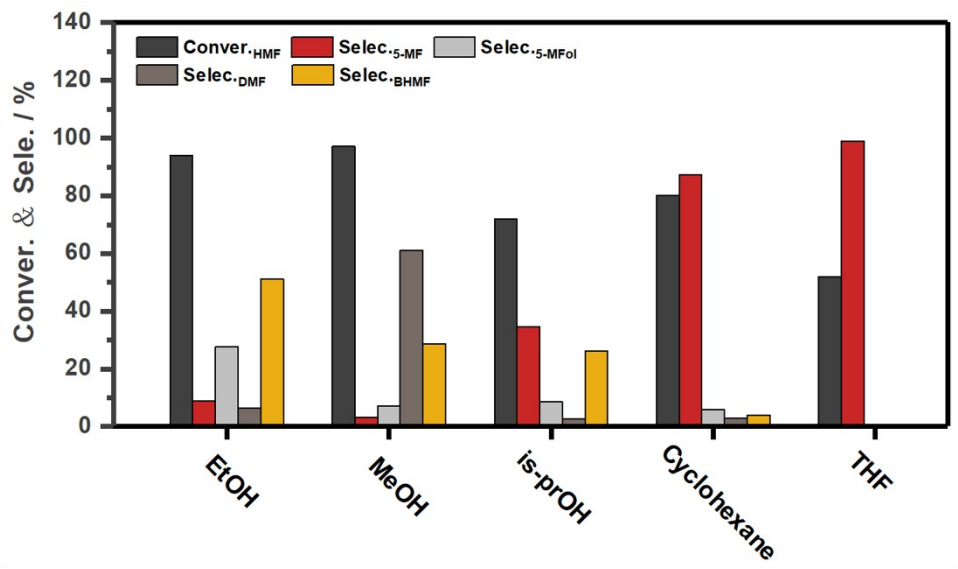


Fig. S1 Solvent screening for hydrolysis of HMF over the $Pt_1$-$CoO_x$#$TiO_2$. Reaction, 30 mg catalyst, 0.2 g HMF, 10 mL solvent, reacted at 200 °C for 3 h.

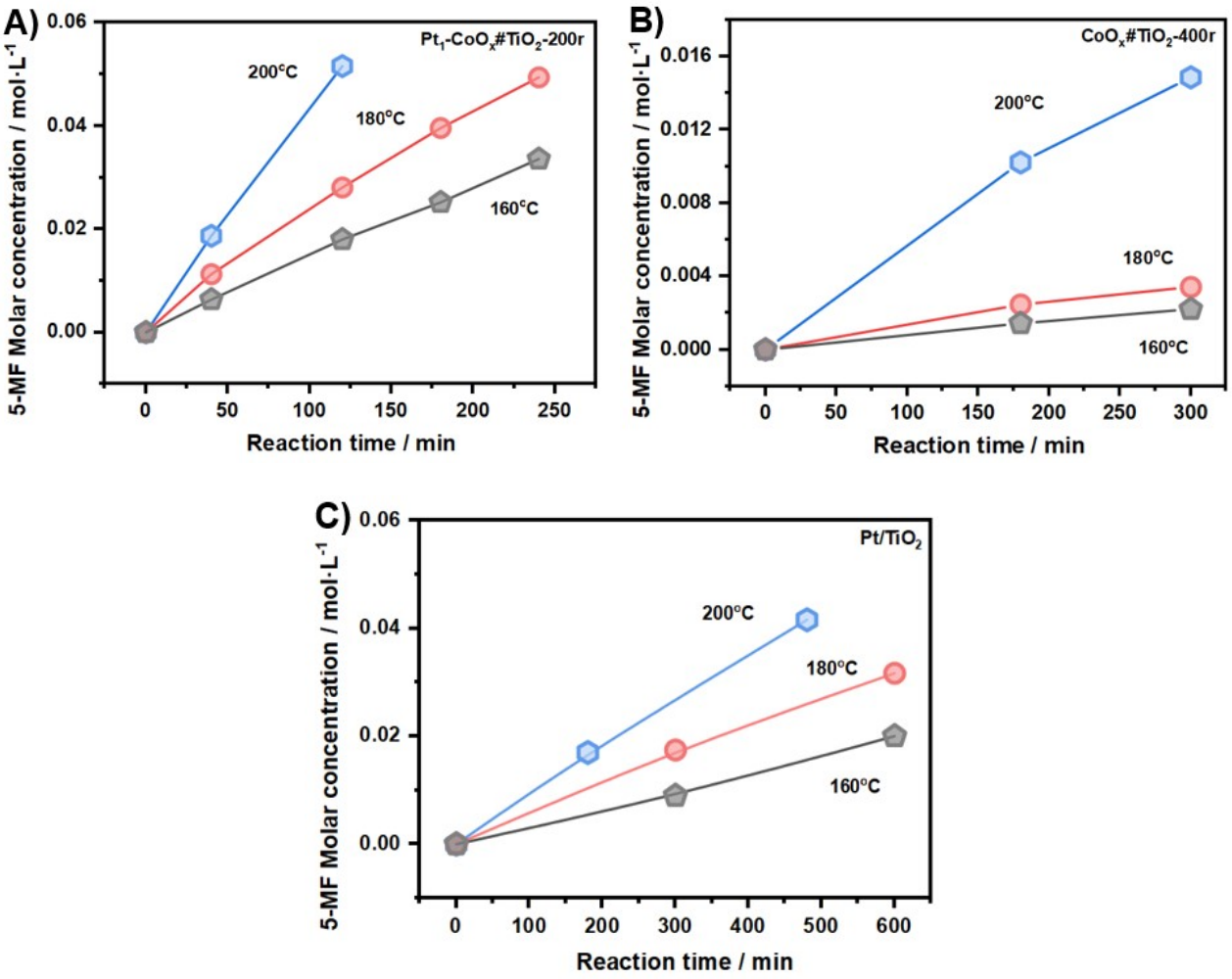


Fig. S2 Hydrogenolysis of HMF as a function of reaction time over different catalyst: (A) $Pt_1$-CoOx#$TiO_2$, (B) $CoO_x$#$TiO_2$, (C) Pt/$TiO_2$.

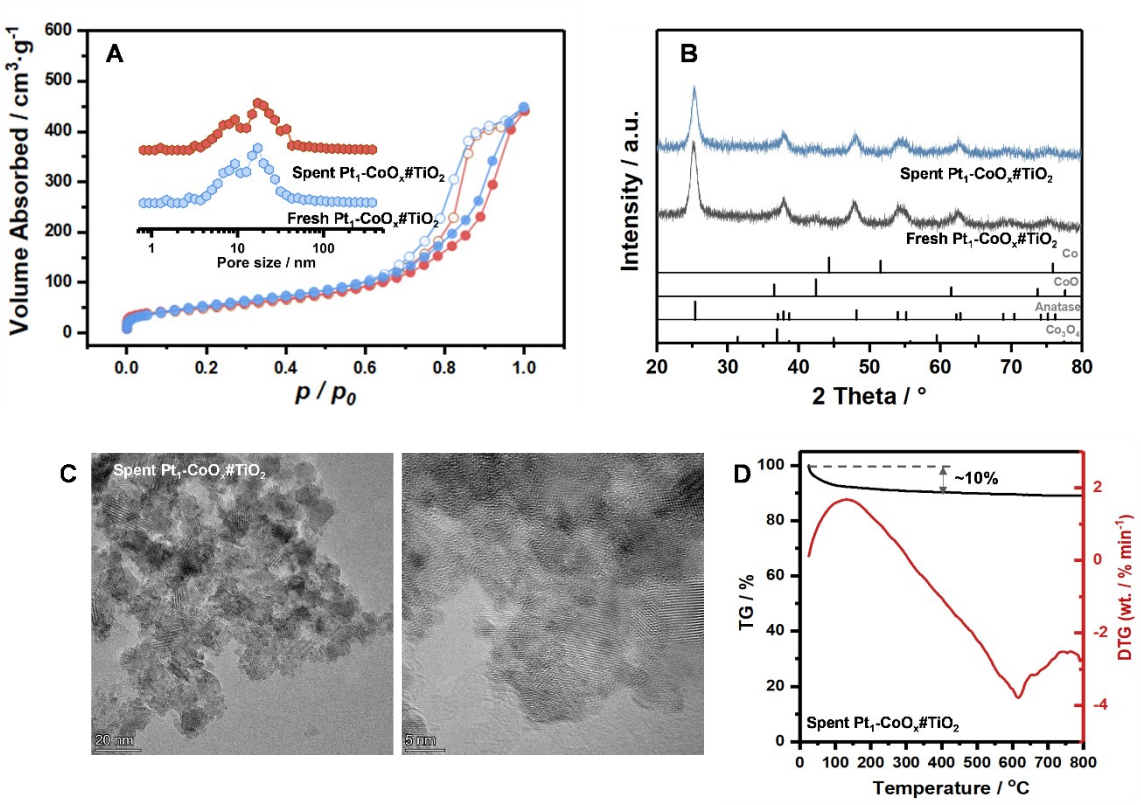


Fig. S3 Structure characterizations of spent $Pt_1$-$CoO_x$#$TiO_2$: (A) Nitrogen sorption, (B) XRD pattern, (C) HRTEM images and (D) TG-DTG plot.

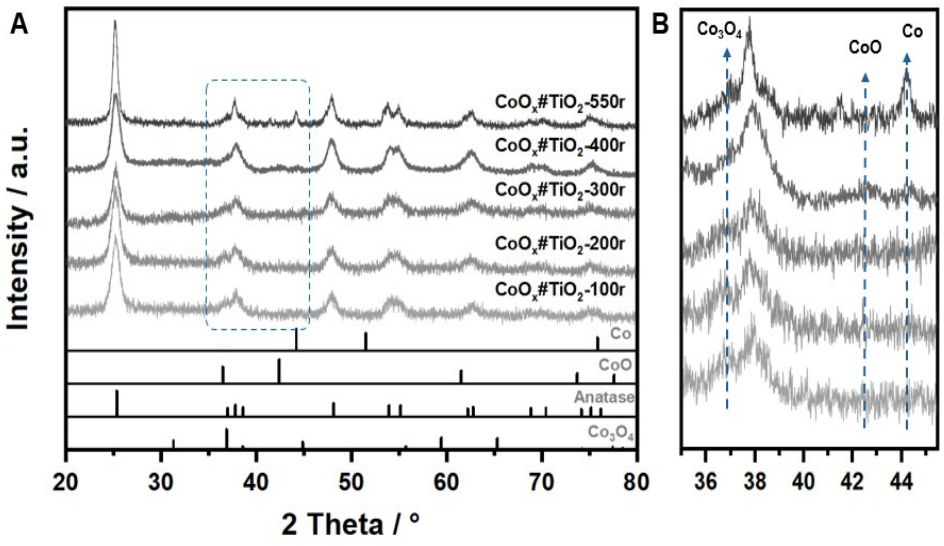


Fig. S4 XRD patterns of a) $CoO_x$#$TiO_2$ reduced at various temperatures.

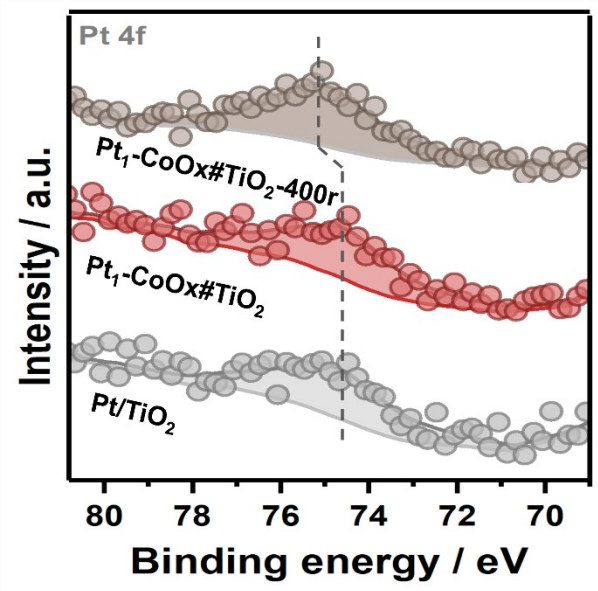


Fig. S5 XPS spectra of Pt 4f for various catalysts

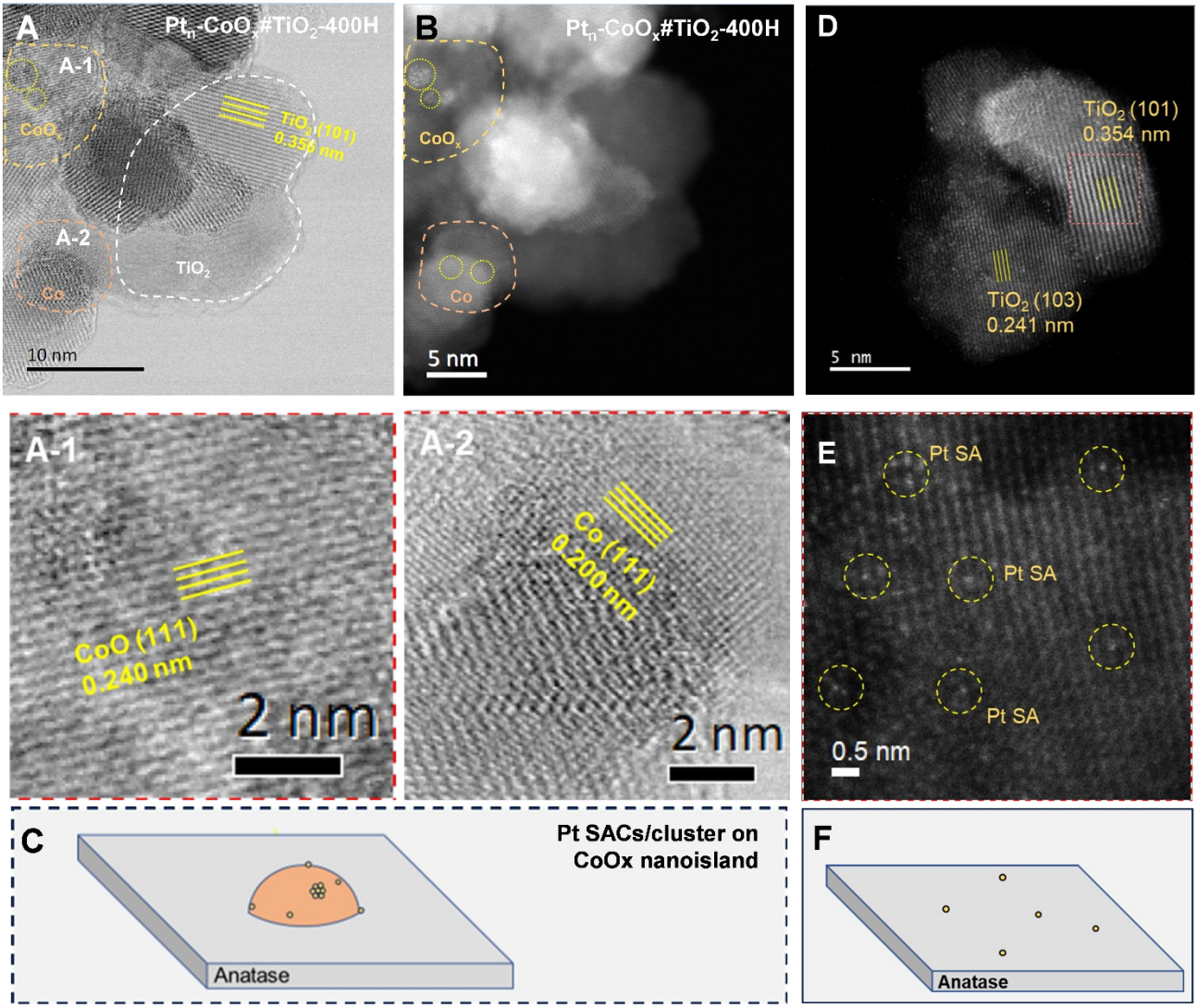


Fig. S6 Aberration corrected HAADF-STEM images showing atomic-scale features of (A-C) $Pt_1$-$CoO_x$/$TiO_2$-400r and (D-F) Pt/$TiO_2$.

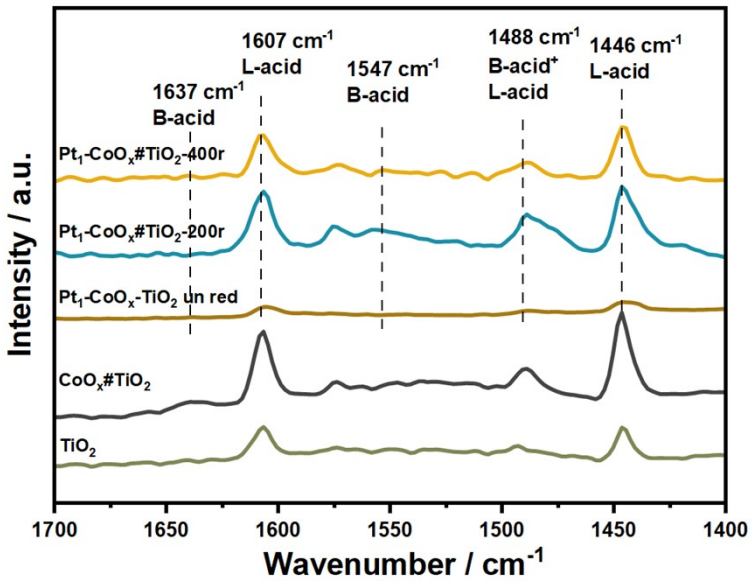


Fig. S7 Pyridine-IR spectrum of various catalysts.

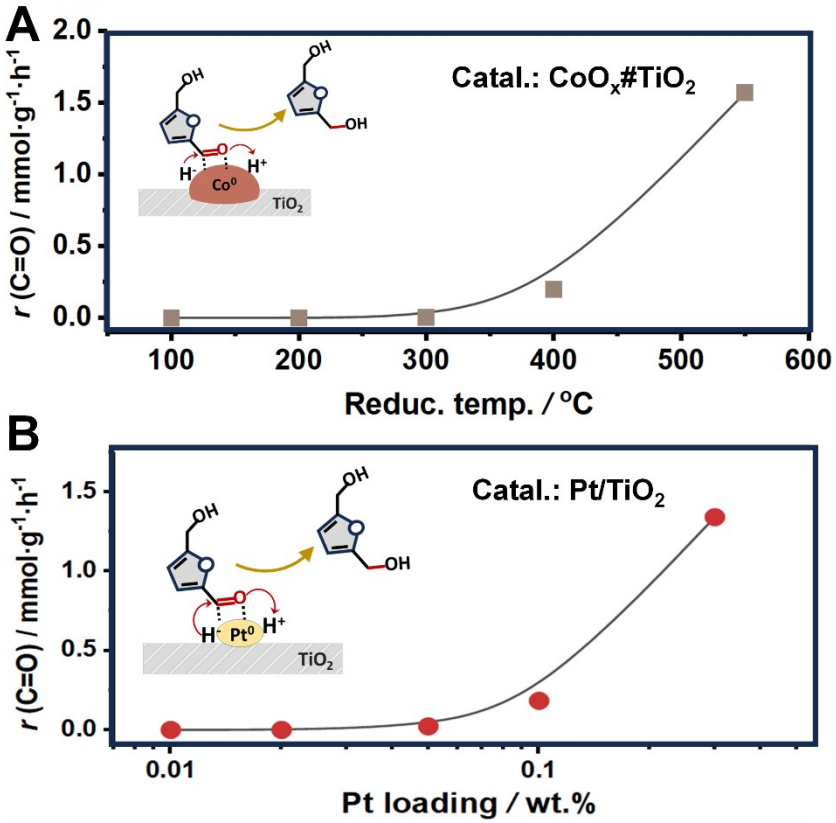


Fig. S8 Aldehyde hydrogenation over $CoO_X$#$TiO_2$ (A)and Pt/$TiO_2$ (B).

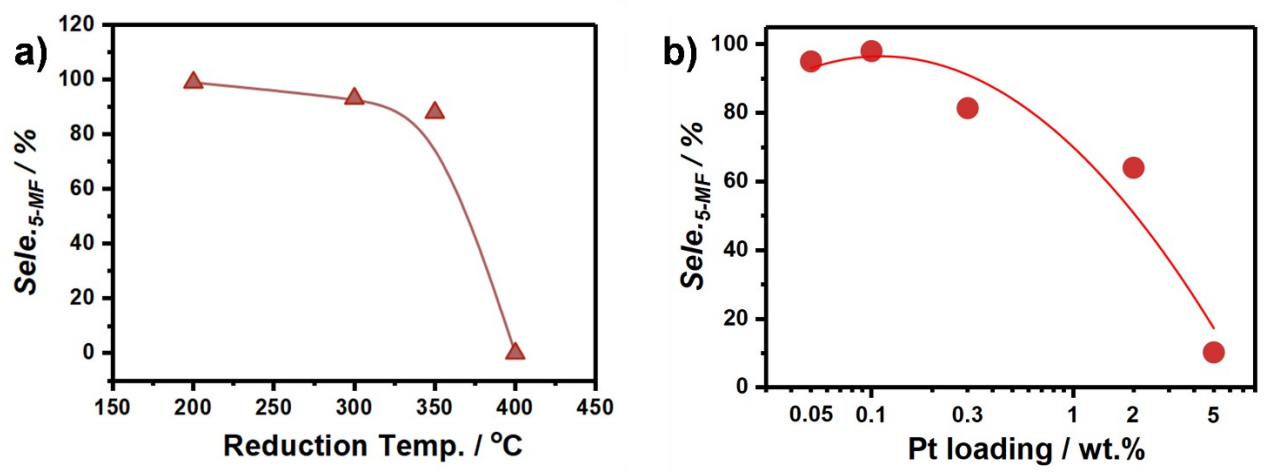


Fig. S9 Hydrodeoxygenation of HMF over the $Pt_1$-$CoO_x$/$TiO_2$ catalyst with various reduction temperatures (a) and Pt loadings (b). The 5-MF selectivity remains above 90% when the reduction temperature is 300° C but begins to decline upon further increasing the temperature. Similarly, when the Pt loading reaches 0.2 wt.% under a reduction temperature of 200° C, the selectivity drops below 90%. We attribute this critical threshold to the temperature-dependent formation of metallic cobalt species and Pt nanoparticle size evolution under different metal loadings.

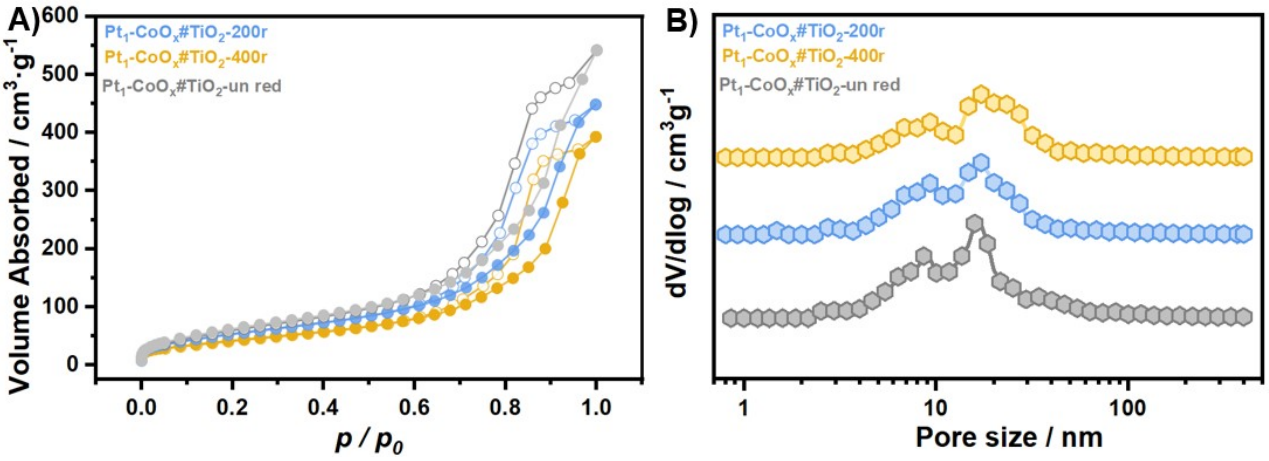


Fig. S10 (A) nitrogen isothermal ads-desorption curves and (B) corresponding pore size distribution plots of $Pt_1$-$CoO_x$#$TiO_2$ reduced with various temperatures.

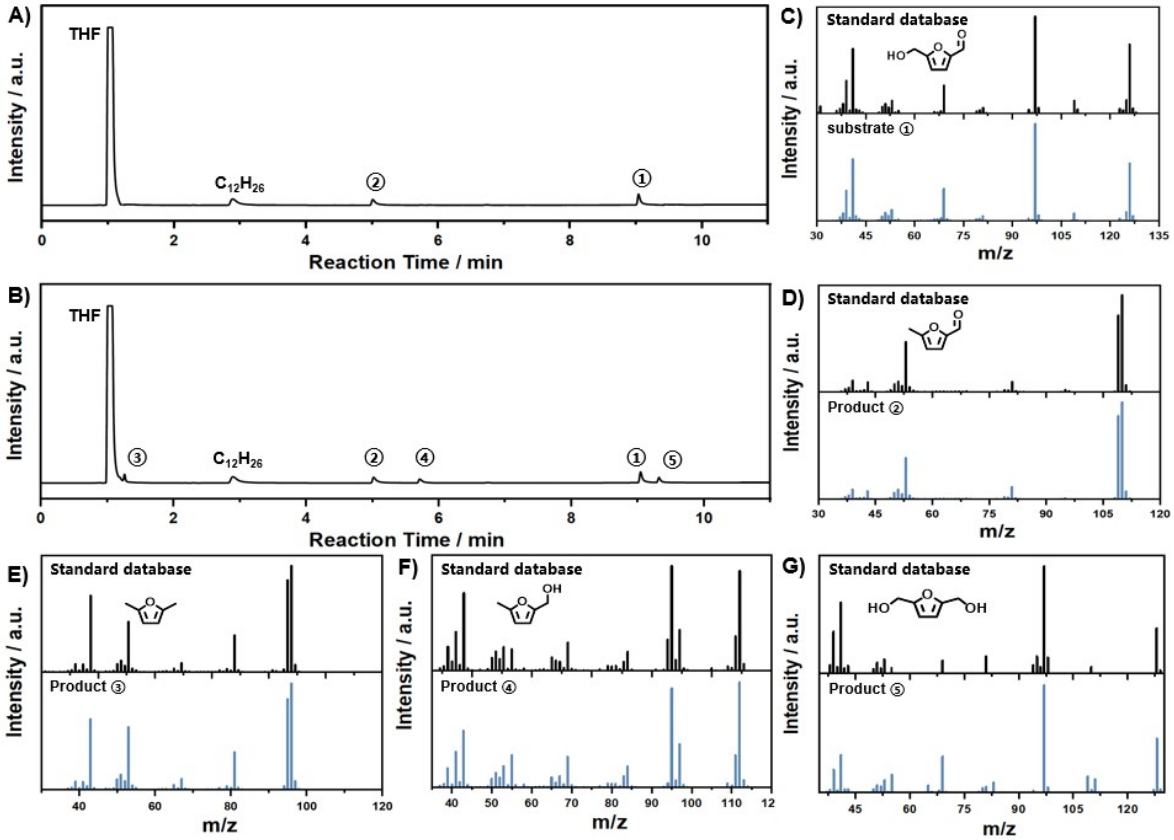


Fig. S11 Representative GC-MASS patterns for HDO of HMF over the different catalysts.

Table S1 Catalyst screening for HDO of HMF into 5-Hydroxymethylfurfural in recent literatures.

| Catalyst | $P_{H2}$ | T/℃ | t/h | Con. /% | Sele.$_{5\text{-MF}}$ /% | Productivity / $mmol_{5\text{-MF}}\ g_{Catal.}^{-1}\ h^{-1}$ | Ref |
|---|---|---|---|---|---|---|---|
| $Pt_1$-$CoO_x$#$TiO_2$ | 1.0 | 160 | 3 | 33 | 100 | 4.40 | This work |
| $Pt_1$-$CoO_x$#$TiO_2$ | 1.0 | 180 | 3 | 37 | 100 | 4.93 | |
| $Pt_1$-$CoO_x$#$TiO_2$ | 1.0 | 200 | 3 | 56.4 | 98 | 7.37 | |
| Au/a-$TiO_2$ | 5 | 230 | 8 | 99.9 | 83.0 | 1.64 | [1] |
| Au/Nb2$O_5$ | 5 | 230 | 8 | 99.9 | 61.2 | 1.21 | [1] |
| Au/Al2$O_3$ | 5 | 230 | 8 | 81.3 | 45.6 | 0.904 | [1] |
| Au/$SiO_2$ | 5 | 230 | 8 | 99.9 | 25.6 | 0.507 | [1] |
| $Pt_1$/$Nb_2O_5$-Ov | 4 | 160 | 4 | 99.9 | 99.9 | 3.74 | [2] |
| Pt@PVP/$Nb_2O_5$ | 3 | 140 | 24 | 99.9 | 92 | 0.287 | [3] |
| Pd-PVP/C (1:2) [a] | 0.5 | 200 | 7.5 | 87 | 90 | 4.14 | [4] |
| FPHS-Pd/C | 4 | 100 | 12 | 100 | 90.1 | 1.77 | [5] |
| Mn_N_Graphene | 1 | 160 | 12 | 99.9 | 92 | 2.30 | [6] |
| Au-4/$TiO_2$@NPC | - | 180 | 1.5 | 100 | 95 | 1.97 | [7] |
| Ni@$NbO_x$ | 4 | 160 | 4 | 94.3 | 91.8 | 2.16 | [8] |
| Pd/$Nb_2O_5$ | 4 | 160 | 4 | 92.9 | 71 | 1.65 | [9] |

[a] The atmosphere is $N_2$.

Table S2 Hydrogenolysis of 5-Hydroxymethylfurfural over various selected catalysts. Reaction, 30 mg catalyst, 10 ml tetrahydrofuran(solvent), 0.2 g HMF, reacted at 200 °C and 1 MPa for 3 h.

| Entry no. | Catalyst | *Conver.* / % | *Selec.* / % | | | | |
|---|---|---|---|---|---|---|---|
| | | HMF  | 5-MF  | DMF  | 5-MFOL  | BHMF  | Others[d] |
| 1 | no catalyst | <1 | — | — | — | — | — |
| 2 | Pristing $TiO_2$ | <1 | — | — | — | — | — |
| 3 | $CoO_x$#$TiO_2$ | 15 | 56.8 | — | — | — | 43.2 |
| 4[a] | $CoO_x$#$TiO_2$ | 26 | 64.7 | 1.4 | 2.6 | 4.2 | 27.1 |
| 5 | Pt/$TiO_2$ | 18.4 | 94.1 | 2.40 | 3.54 | — | — |
| 6[b] | CoO NPs | 99 | 53 | 6.4 | 7.2 | 5.1 | 28.3 |
| 7 | $Pt_1$-$CoO_x$#$TiO_2$ | 42 | 69 | 6.0 | 9.05 | 15.6 | 0.35 |
| 8[c] | $Pt_1$-$CoO_x$#$TiO_2$ | 44 | 92 | — | — | — | |

[a] $CoO_x$#$TiO_2$-400r was reduced by hydrogen at 400 °C; [b] CoO nanoparticles (NPs) were purchased from Macklin Agent Cop.; [c] the 6th recycle run after regeneration; [d] others mainly refer to side products derived from aldol condensations, such as 4-(2-furyl)-3-buten-2-one, 1,4-pentadien-3-one, 1,5-di-2-furanyl, etc[10].

Table S3 Sample specifications for various catalysts.

| **Catalyst** | **$S_{BET}$ / $m^2g^{-1}$** | ***Pt loading wt.%*** | ***Co loading wt.%*** | ***$D_{pore}$* / nm** |
|---|---|---|---|---|
| $Pt_1$-$CoO_x$#$TiO_2$-un red | 241 | 0.1 | 11 | 9.58 |
| $Pt_1$-$CoO_x$#$TiO_2$-200r | 207 | 0.1 | 11 | 9.73 |
| $Pt_1$-$CoO_x$#$TiO_2$-400r | 160 | 0.1 | 11 | 10.7 |

The mass percentages of Pt and Co were determined by ICP analysis.

Table S4 Sample specifications over different catalyst.

| Sample | $H_2$ ads. / mmol $g^{-1}$ [a] | Acidity /mmol $g^{-1}$ [b] |
|---|---|---|
| $Pt/TiO_2$ | 0.31 | 1.28 |
| $CoO_x\#TiO_2$ | 0.21 | 2.27 |
| $Pt_1\text{-}CoO_x\#TiO_2$ | 1.13 | 4.33 |
| $Pt_1\text{-}CoO_x\#TiO_2\text{-}400r$ | 2.6 | 4.54 |

[a] Hydrogen adsorption amount was calculated by data derived from $H_2$-TPD test;

[b] Acidity was calculated by data derived from $NH_3$-TPD test;

Table S5 Substrate scope over the $Pt_1$-$CoO_x$#$TiO_2$. Reaction, 0.1 g substrate, 30 mg catalyst, 200 °C, 2 MPa, reacted for 3h. For furan compounds (e.g., furfural, 2-methyl furfural, and their corresponding alcohols), the catalyst demonstrated high dehydroxylation activity and low aldehyde hydrogenation activity; yet, this distinct activation behavior toward aldehydes versus alcohols was far less pronounced in benzene-derived aromatic substrates.

| Entry No. | Substrate | Conver. (%) | Product | Selec. (%) |
|---|---|---|---|---|
| 1 | 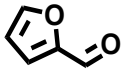 | 2 | 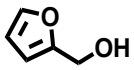 | - |
| 2 | 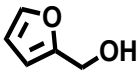 | 67 |  | >99 |
| 3 | 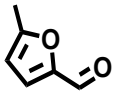 | <1 | 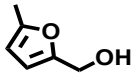 | - |
| 4 | 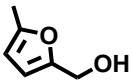 | 59 |  | 59 |
| 5 | 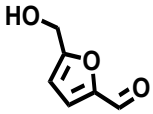 | 53 | 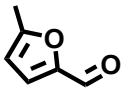 | 98 |
| 6a | 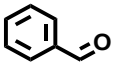 | 41 | 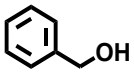 | 76 |
| 7a | 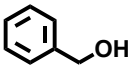 | 28 |  | >99 |
| 8 | 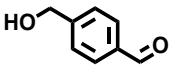 | >99 | 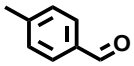 | 38 |
| 9 | 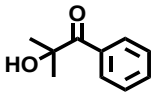 | <1 | 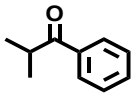 | - |
| 10b | 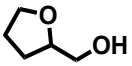 | 3 |  | >99 |
| 11c | 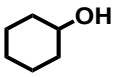 | 10 |  | >99 |
| 12 |  | <1 |  | - |

[a] reaction at 150 °C; [b] reaction at 3.8 MPa $H_2$; [b] reaction for 5 h.

## References


1. L. Dong, J. Morales-Vidal, L. Mu, L. Li, N. López, J. Pérez-Ramírez and Z. Chen, *Applied Catalysis B: Environmental*, 2023, **335**, 122893.
2. S. Li, M. Dong, J. Yang, X. Cheng, X. Shen, S. Liu, Z.-Q. Wang, X.-Q. Gong, H. Liu and B. Han, *Nature*

*Communications*, 2021, **12**, 584.

3. S. Li, J. D., B. Zhang, Y. Liu, Q. Mei, Q. Meng, M. Dong, J. Du, Z. Zhao, L. Zheng, B. H. Han, M. Zhao and H. Liu, *Acta Phys. -Chim. Sin.*, 2022, **38**, 2206019-.
4. G. Sun, J. An, H. Hu, C. Li, S. Zuo and H. Xia, *Catalysis Science & Technology*, 2019, **9**, 1238-1244.
5. Q. Deng, J. Lu, G. Sheng, Y.-C. Zhang, J. Wang, Z. Zeng, T. Yoskamtorn and S. C. Edman Tsang, *ACS Catalysis*, 2023, **13**, 14356-14366.
6. M. S. Ahmad, Y. Nagata, K. Masumoto, Y. Inomata, K. Hatakeyama, A. T. Quitain, A. Shotipruk and T. Kida, *Molecular Catalysis*, 2024, **553**, 113787.
7. J. Zhang, Z. Wang, M. Chen, Y. Zhu, Y. Liu, H. He, Y. Cao and X. Bao, *Chinese Journal of Catalysis*, 2022, **43**, 2212-2222.
8. Y. Liu, H. Yuan, B. Zhang, L. Zhang, Q. Xu, M. Dong, T. Wang, X. Cheng, H. Qi, Z. Zhao, L. Chen, B. Su, B. Han and H. Liu, *ACS Sustainable Chemistry & Engineering*, 2024, **12**, 16202-16211.
9. Y. Liu, B. Zhang, J. Xia, M. Douthwaite, M. Dong, H. Yuan, X. Cheng, S. Luan, Y. Wu, Z. Zhao, J. Tai, L. Chen, B. Su, B. Han and H. Liu, *Chemical Engineering Journal*, 2024, **479**, 147687.
10. N. S. Biradar, A. M. Hengne, S. S. Sakate, R. K. Swami and C. V. Rode, *Catalysis Letters*, 2016, **146**, 1611-1619.